Published on 03 February 2015. Downloaded by Changchun Institute of Optics, Fine Mechanics and Physics, CAS on 29/05/2016 11:47:40.

Nanoscale

ROYAL SOCIETY OF CHEMISTRY

PAPER

View Article Online
View Journal | View Issue

Cite this: *Nanoscale*, 2015, **7**, 4522

Optimized growth of graphene on SiC: from the dynamic flip mechanism

Dandan Wang,[a,b] Lei Liu,*[a] Wei Chen,*[c,d] Xiaobo Chen,[e] Han Huang,[c,f] Jun He,[f] Yuan-Ping Feng,[c] A. T. S. Wee[c] and D. Z. Shen[a]

Received 5th December 2014,
Accepted 2nd February 2015

DOI: 10.1039/c4nr07197b

www.rsc.org/nanoscale

Thermal decomposition of single-crystal SiC is one of the popular methods for growing graphene. However, the mechanism of graphene formation on the SiC surface is poorly understood, and the application of this method is also hampered by its high growth temperature. In this study, based on the *ab initio* calculations, we propose a vacancy assisted Si–C bond flipping model for the dynamic process of graphene growth on SiC. The fact that the critical stages during growth take place at different energy costs allows us to propose an energetic-beam controlled growth method that not only significantly lowers the growth temperature but also makes it possible to grow high-quality graphene with the desired size and patterns directly on the SiC substrate.

1. Introduction

Due to its extremely high carrier mobility,[1–3] graphene has attracted a lot of attention as a strong contender for the channel material, replacing silicon, in the next generation high-speed and low power consumption optoelectronic devices.[4,5] However, to meet the industrial requirement, graphene with large domains and good homogeneity must be produced in large quantities. To date, a number of techniques have been proposed for the growth of high-quality graphene, for example, mechanical exfoliation of pyrolytic graphite,[1,2] chemical vapor deposition (CVD) on a metal substrate,[6,7] chemical reduction of graphene oxide films,[8,9] thermal decomposition of single-crystal SiC[10–13] *etc*. Among these growth methods, CVD seems to be the most promising technique for producing good-quality graphene on a large scale. However, to fabricate graphene-based electronic devices, these graphene layers have to be transferred from the metal substrate to a dielectric substrate, which may result in the contamination, wrinkling, and breakage of the samples,[14] leading to degradation of their electrical properties.[15]

Compared to CVD growth of graphene on a metal substrate, graphene grown on SiC does not need to be transferred to another substrate since SiC itself is a good dielectric. This would help avoid the problems encountered during the sample transferring process mentioned above. Furthermore, being a wide gap material, the 6H-SiC substrate has its clear advantages. For example, electronic circuits can be fabricated with a much lower leakage current. As early as in the 1970s, SiC(0001) surfaces were found to be easily "covered" by a layer of graphite, which is typically monocrystalline on a Si-rich surface but polycrystalline on a C-rich surface.[16] More recently, it was demonstrated that large crystalline domains of graphene can be grown on SiC,[10,11] and single domains as large as $5 \times 500\ \mu m^2$ have been observed.[12]

Despite these merits and successes of growing graphene on SiC, the high growth temperatures (above 1000 °C) make it formidable for large-scale practical applications in graphene-based electronics. Recently, Ouerghi *et al.* successfully grew large-scale uniform monolayer and bilayer graphene on off-axis 6H-SiC(0001) substrates.[12] Compared to the normal SiC (0001) surface, off-axis growth creates more dangling bonds per unit area which favors sublimation of Si atoms. Similarly, de Heer and coworkers reported selective epitaxial growth of graphene nanoribbons on templated SiC substrate by heating the sample above 1200 °C. The growth of graphene ribbons was found to initiate from the step bunchings that can form nanofacets with weaker bonding of Si atoms.[17,18] Nevertheless, these synthesis temperatures of graphene layers on the SiC substrate are still rather high (~1300 °C), which makes it

[a]State Key Laboratory of Luminescence and Applications, Changchun Institute of Optics, Fine Mechanics and Physics, Chinese Academy of Sciences, No. 3888 Dongnanhu Road, Changchun, 130033, People's Republic of China. E-mail: liulei@ciomp.ac.cn
[b]University of Chinese academy of sciences, Beijing 100039, People's Republic of China
[c]Department of Physics, National University of Singapore, 2 Science Drive 3, 117542, Singapore. E-mail: phycw@nus.edu.sg
[d]Department of Chemistry, National University of Singapore, 3 Science Drive 3, 117543, Singapore
[e]University of Missouri - Kansas City, Department of Chemistry, Kansas City, MO 64110, USA
[f]School of Physics and Electronics, Hunan Key Laboratory for Super-Microstructure and Ultrafast Process, Central South University, Changsha 410083, China

This journal is © The Royal Society of Chemistry 2015

Published on 03 February 2015. Downloaded by Changchun Institute of Optics, Fine Mechanics and Physics, CAS on 29/05/2016 11:47:40.

difficult to integrate SiC wafer into the currently available technology for silicon-based electronics.

The high growth temperature originates from the rather strong Si–C bonds in SiC. The bonding energy is roughly 2.86 eV per Si–C bond[19] and a very high amount of energy or temperature is required to break the bond to enable Si sublimation on SiC surfaces. Naturally, if alternative mechanisms can be found that involve breaking of less number of Si–C bonds in the process, graphene would be grown on SiC at a lower temperature with better quality. This has been actively pursued in recent years. Attempts have been made by several groups to prepare graphene on the SiC substrate by energy electron beam or laser beam irradiation. To start with, Huang *et al.* obtained epitaxial graphene within three monolayers on a 4H-SiC substrate using pulsed electron irradiation at 320–530 °C.[20] They demonstrated that the sublimation of surface silicon atoms is activated by the energy transferred from the electrons to the topmost surface atoms of the SiC substrate. Subsequently, Go *et al.* reported random rotation of epitaxial graphene layers on a 6H-SiC substrate by continuous e-beam irradiation at ~670 °C.[21] Furthermore, Dharmaraj *et al.* demonstrated the possibility of precise control of an E-beam over the SiC substrate for uniform graphene growth.[22] Meanwhile, Lee *et al.* were able to synthesize graphene for the first time by heating only the SiC surface and keeping the substrate at room temperature using a KrF excimer laser.[23] Later, Yannopoulos *et al.* reported the growth of low-strain graphene films on the SiC substrate using an infrared CO_2 laser as the surface heating source which promotes cleavage of Si–C bonds and evaporation of Si atoms from the SiC surface.[24] Therefore, the energy assisted approaches seem promising for lowering the growth temperature of graphene on the SiC substrate. The remaining issues are a high concentration of domain boundaries and related misalignment of crystals in different domains, as well as a large amount of defected areas in samples grown using such irradiation methods. Thus, eliminating grain boundaries to reduce carrier scattering, controlling crystal quality and size, and patterning graphene on the SiC substrate are new challenges and bring new critical issues to electronics based on graphene on the SiC substrate.

Growing high-quality graphene and engineering its structure on SiC rely on a good understanding of the dynamic process of graphene formation. To date, many studies have been carried out to investigate the atomic structure of graphene and the dynamic process of its growth on global heated SiC above 1000 °C. Back in 2005, Chen *et al.* investigated the atomic structure of a carbon nanomesh on the 6H-SiC(0001) surface by scanning tunneling microscopy (STM) and low energy electron diffraction (LEED). A 6 × 6 reconstruction model was proposed to explain the STM images observed during the growth process.[25] In 2008, Emtsev *et al.* proposed a $(6\sqrt{3} \times 6\sqrt{3})R30°$ reconstruction as the precursor of graphene growth on the Si-terminated SiC surface.[26] Meanwhile, Huang *et al*. demonstrated that epitaxial graphene grows *via* a bottom-up mechanism on the SiC surface.[27] In 2011, using isotopic labelling of ^{13}C, Hannon *et al.* directly observed the graphene growth mode on Si- and C-terminated SiC(0001) surfaces, and confirmed that new layers of graphene form underneath the existing ones during SiC decomposition at high temperature.[28] Based on the energetics *via* the first-principles density functional theory (DFT) calculations, Kageshima *et al.* provided many suggestions about graphene formation on the SiC(0001) surface.[29] They reported that the Si terminated surface is important for the epitaxial growth of thin flat graphene sheets. By using DFT calculations, Kim *et al.* showed that a quasi-periodic 6 × 6 domain pattern emerges out of a larger commensurate $(6\sqrt{3} \times 6\sqrt{3})R30°$ periodic interfacial reconstruction which accounts for the STM and LEED observations.[30] More recently, Inoue *et al.* discussed the role of pentagonal and heptagonal rings during the growth of graphene-like carbon clusters on the SiC(0001) substrate, based on findings of their DFT calculations.[31] Moreover, the impact of the substrate steps on graphene growth by decomposition of SiC (0001) was also theoretically studied by first-principles calculations[32] and by DFTB/MD atom-by-atom simulations.[33] A further study by Hwang *et al.* suggested that graphitization of SiC during repeated laser exposures is similar to thermal graphitization, *i.e.*, silicon atoms are sublimated and the residual carbon atoms gradually form graphene islands.[34] Similarly, Huang *et al.* pointed out that the carbon-rich layers created by Si sublimation within an effective penetration depth of the electron beam collapse to form epitaxial graphene as that which happens in a heated SiC substrate.[20] Despite these advances, formation of graphene on the SiC substrate assisted by a low energy electron beam or laser irradiation is not yet fully understood. The dynamics of Si sublimation, *i.e.*, how Si atoms initially break away from the SiC surface and how the neighboring C atoms respond, to eventual formation of graphene, is poorly understood. A complete understanding of this dynamic process is essential for precise control of irradiation parameters and the ultimate growth of high-quality graphene under practical experimental conditions.

In this work, with the help of *ab initio* calculations, we systemically investigate the growth mechanism of graphene on SiC by simulating its surface morphology at critical growth stages. Our calculations demonstrate that the optimal growth path for graphene consists of initial formation of surface Si vacancies, vacancy assisted flipping of Si–C pairs, sublimation of Si atoms and subsequent formation of C clusters, propagation of Si sublimation, aggregation of C atoms into graphene flakes, and eventual delamination and rotation of single-layer graphene, forming the $(6\sqrt{3} \times 6\sqrt{3})R30°$ surface. Based on the different energies involved in various stages of the growth process, we systematically propose a low temperature approach, controlled by an energetic-beam, for growing high-quality graphene with desired size and patterns on the SiC substrate.

2. Computational method

Our theoretical calculations are based on DFT within the Perdew–Burke–Ernzerhof (PBE) generalized gradient approxi-

This journal is © The Royal Society of Chemistry 2015

Published on 03 February 2015. Downloaded by Changchun Institute of Optics, Fine Mechanics and Physics, CAS on 29/05/2016 11:47:40.

mation[35] and the projected augmented wave (PAW) method as implemented in the Vienna *ab initio* simulation package (VASP).[36,37] A special *K*-point sampling with a *k*-point separation of <0.05 $Å^{-1}$ is applied for the Brillouin-zone integration. The cutoff energy for the plane wave basis set is 400 eV, and a vacuum region of 15 Å is used in building the slab models in which dangling bonds at the bottom are saturated by H atoms. Atomic positions are relaxed until their residual forces are less than 0.005 eV $Å^{-1}$. The lattice parameters obtained for the relaxed bulk 6H-SiC, a = 3.10 Å and c = 15.16 Å, are in good agreement with the experimental values (3.08 and 15.12 Å, respectively).[38]

3. Results and discussion

3.1. The $(\sqrt{3} \times \sqrt{3})R30°$ reconstruction

Experimentally graphene can be synthesized on different SiC surfaces at high temperature under ultrahigh vacuum. In the present study, we focus on the growth of graphene on the Si-terminated 6H-SiC(0001) surface. This is because this surface can be realized at relatively lower temperatures with well-defined early and intermediate states. It is known that for this surface, annealing up to 900–1000 °C in UHV, following chemical cleaning and passivation of the surface, results in the $(\sqrt{3} \times \sqrt{3})R30°$ reconstruction, and further annealing above 1000° causes depletion of Si and graphitization of the surface, leading to the $(6\sqrt{3} \times 6\sqrt{3})R30°$ reconstruction.[39] The $(\sqrt{3} \times \sqrt{3})R30°$ reconstruction of 6H-SiC(0001), characteristic of the preliminary growth stage, has been generally observed by many groups during annealing prior to graphene growth.[25,27] Bermudez *et al.* further showed that the $(\sqrt{3} \times \sqrt{3})R30°$ reconstruction indeed involves an ordered arrangement of Si vacancies.[40] The lack of Si does provide an important hint that Si sublimation plays a key role in the dynamic process of graphene growth on SiC. It also discounted earlier models based on Al, Ga, In, Pb,[41] Si or C[39] adatoms which fail to explain the role of the $(\sqrt{3} \times \sqrt{3})R30°$ phase.

In order to understand high-temperature Si sublimation, it is instructive to examine the energetics of the clean SiC(0001) surface and the $(\sqrt{3} \times \sqrt{3})R30°$ morphology. For the clean surface, we identify a $(\sqrt{3} \times \sqrt{3})R30°$ reconstruction which is more stable and its total energy is 0.31 eV lower than that of the relaxed (1 × 1) surface. Fig. 1(a) and (b) show the side views of these two surfaces, respectively. The main difference between the two surfaces lies in the positions of the Si atoms at the surface layer. In the bulk-truncated (1 × 1) surface, all Si atoms in the top surface layer are in the same plane and have uniform Si–C bond lengths, while in the reconstructed $(\sqrt{3} \times \sqrt{3})R30°$ surface two of the three Si atoms in each unit cell relaxed inward by 0.20 Å and the third one was raised by 0.43 Å. This reconstruction can be ascribed to the general model for (111) surfaces of zinc-blende semiconductors as proposed by Haneman.[42] In the reconstructed surface, counting along closed-spaced rows, every third atom is raised with respect to its neighbors to relieve the surface strain due to dangling bonds. To discern this $(\sqrt{3} \times \sqrt{3})R30°$ reconstruction from the 1 × 1 surface, we present in Fig. 1(c) and (d) the simulated STM images of the two surfaces obtained using the Tersoff–Hamann approach.[43] Compared to the Si atoms in the 1 × 1 surface (Fig. 1(c)), one-third of the Si atoms in the top layer of the $(\sqrt{3} \times \sqrt{3})R30°$ reconstructed surface move outward by 0.43 Å and the other two-thirds move inward by 0.20 Å resulting in the big and the small white dots seen in Fig. 1(d).

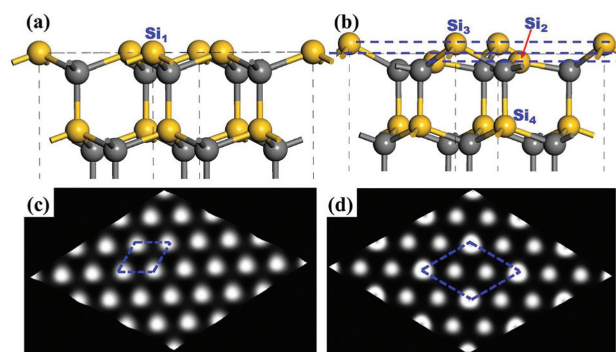

Fig. 1 Models and simulated STM images of the Si-terminated 6H-SiC (0001) surfaces. (a) Side view of the unreconstructed 1 × 1 surface. (b) Side view of the reconstructed $(\sqrt{3} \times \sqrt{3})R30°$ surface. (c) STM image of the unreconstructed surface. (d) STM image of the reconstructed surface. The yellow and dark grey balls represent Si and C atoms, respectively, and the blue dotted lines indicate the unit cells of the two surfaces.

The corrugation of the $(\sqrt{3} \times \sqrt{3})R30°$ surface results directly from the reconstruction of the Si–C bonds in the top layer to relieve the surface strain. In comparison, the Si–C bond length and the C–Si–C bond angle respectively are 1.90 Å and 109.58° in bulk SiC, 1.86 Å and 112.76° for Si atoms in the top layer of the 1 × 1 surface (Si_1), 1.82 Å and 117.36° for the lower Si atoms (Si_2) and 2.00 Å and 100.33° for the upper Si-atoms in the top layer of the $(\sqrt{3} \times \sqrt{3})R30°$ reconstructed surface (Si_3). Naturally, the stretched Si–C bonds would have lower binding energy compared to the contracted ones. Based on results of our calculations, the energy required to free Si_1, Si_2, and Si_3 from their C neighbors, *i.e.* to move the Si atoms far away from the surface, is about 8.00, 13.68, and 7.46 eV, respectively, which implies that, in comparison with the 1 × 1 surface, the $(\sqrt{3} \times \sqrt{3})R30°$ reconstruction favors the initial Si sublimation by about 0.54 eV per atom. That accounts for the presence of Si vacancies[40] in the $(\sqrt{3} \times \sqrt{3})R30°$ reconstructed surface.

3.2. The flip mechanism

Graphene has been known to form underneath existing layers during its high-temperature growth on SiC(0001),[27,44,45] but so far there has been no quantitative model for the formation of the initial top graphene layer. Herein, we propose a bond flip mechanism to account for the details of the dynamic growth of graphene on SiC(0001), from the initial formation of Si vacancies (V_{Si}), to eventual formation of the $(6\sqrt{3} \times 6\sqrt{3})R30°$ surface, covered by a single layer of graphene.

 This journal is © The Royal Society of Chemistry 2015

Published on 03 February 2015. Downloaded by Changchun Institute of Optics, Fine Mechanics and Physics, CAS on 29/05/2016 11:47:40.

Although the $(\sqrt{3}\times\sqrt{3})R30°$ reconstruction favors sublimation of the 1/3 of the Si atoms in the top layer (Si_3), essentially all Si atoms in the two surface layers of the SiC(0001) surface must be removed to create a monolayer of carbon using the residual carbon atoms. However, removing the Si_2 atoms in the surface layer and Si atoms in the second layer (Si_4) would involve breaking of either three contracted sp^2-like or four sp^3 bonds per atom, requiring more energy or higher temperature. For example, in the presence of a V_{Si} at the Si_3 site, the three carbon atoms around this surface V_{Si} contract slightly toward the surface Si atoms (Si_2) with which they are bonded. This contraction of the C–Si bond makes it harder for sublimation of the Si_2 atoms than Si_3. The energy required to remove the Si_2 atom is >1.0 eV more than that required to remove Si_3. Instead of removing these Si atoms, we consider an alternative mechanism of swapping a carbon atom in the top layer with the Si atom directly below it in the second layer, or flipping a C–Si bond. If this is possible, then the Si cluster in the top layer would allow easier sublimation of Si and, at the same time, a carbon cluster would form in the second layer. This process is illustrated in Fig. 2. We also compare the energetics of bond flipping before (Fig. 2(a)) and after (Fig. 2(b)) the removal of the topmost Si atom (Si_3) from the $(\sqrt{3}\times\sqrt{3})R30°$ surface. With the elastic band method, we can estimate the minimum energy path and energy barrier of the bond flip process. As shown by the energy profiles in Fig. 2(c), much less energy is required to flip the bond in the presence of the surface Si vacancy. Therefore, we can conclude that this is a surface vacancy induced bond flipping process and the surface V_{Si} can significantly reduce the energy barrier for flipping the Si–C bond, from 5.6 to 2.4 eV. Once the vacancy-assisted bond flipping is complete, the swapped Si atom (Si_4) bonds to two Si atoms (Si_2), forming a labile $–Si_2–Si_4–Si_2–$ chain, whereas the swapped C atom bonds to three C atoms forming a Y-shaped C_4 cluster which can serve as a nucleus for the growth of graphene nanoflakes.

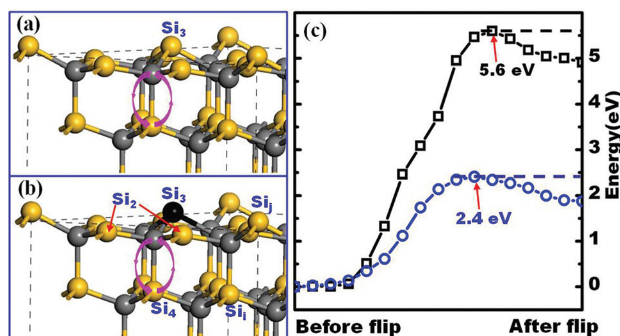

Fig. 2 Models showing the bond flip processes on (a) the defect free (without Si vacancy) and (b) in the presence of a Si vacancy created by sublimation of Si_3, respectively, of the $(\sqrt{3}\times\sqrt{3})R30°$ reconstructed surface, and (c) the corresponding minimum energy paths (black square for model (a) and blue circle for model (b)). The black ball indicates the Si vacancy created by sublimation of Si_3. The pink arrows show schematically the exchange of the Si–C pairs.

Compared to the initial sublimation of Si_3, the three Si atoms in the $–Si_2–Si_4–Si_2–$ chain can be removed more easily. Based on our calculations, it takes about 5.5 eV to free the central Si_4 atom and thereafter 5.7 eV to release the Si_2 atoms. The sublimation of the $–Si_2–Si_4–Si_2–$ chain creates vacancies next to the Si atoms in the second layer (Si_i) and its neighboring C atoms in the top layer. Flips of these Si–C bonds are again facilitated by these vacancies, creating similar three-atom chains, which favors sublimation of atoms Si_i, Si_j, and so on. As a result, the Si sublimation propagates in the top SiC layer, and C atoms aggregate underneath it, leading to the formation of a graphene nanoflake. The growth of a layer of graphene is complete when the nanoflakes join together and cover the entire SiC surface.

In real graphene growth, there would be many Si vacancies triggered randomly on the Si-terminated SiC surfaces during its preheating stage following the formation of the $(\sqrt{3}\times\sqrt{3})R30°$ surface. Go *et al.* also observed many small graphene islands distributed randomly on the SiC substrate during the early stage of electron beam irradiation.[21] Thus, before the eventual formation of the $(6\sqrt{3}\times 6\sqrt{3})R30°$ phase of epitaxial graphene layer, intermediate states will exist in the form of irregular structures full of vacancies, flips, and small domains of Si and C. During the epitaxial growth of graphene on SiC(0001),[25,27] such irregular intermediate surfaces have indeed been observed around the $(\sqrt{3}\times\sqrt{3})R30°$ patterns by STM as shown in Fig. 3(a). In Fig. 3(b), we present a simulated STM image of a SiC(0001) surface with arbitrarily distributed

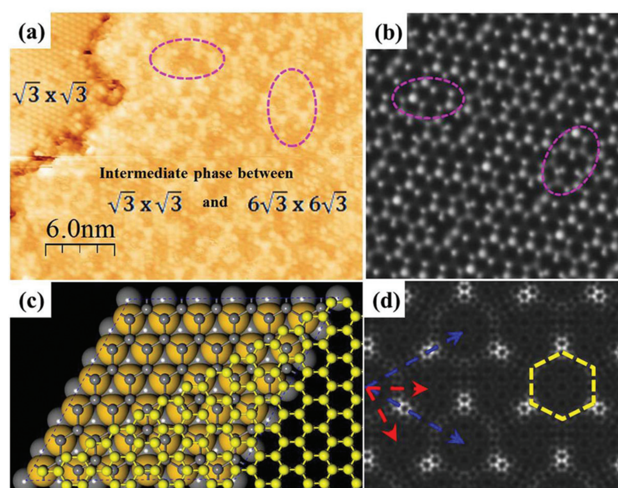

Fig. 3 (a) Experimental filled state STM image of the SiC (0001) surface at a bias voltage of 2.0 V, showing the immediate irregular phase. (b) Simulated STM image of the SiC (0001) surface with randomly distributed bond flips. The purple elliptic curves in (a) and (b) denote the consistent parts between experimental and simulated STM images. (c) Model showing a transient (1 × 1) carbon layer formed by residual carbon atoms after sublimation of Si atoms in the top two layers (small dark grey balls) and orientation of the grown graphene (yellow balls). The intermediate carbon layer is commensurate with the SiC surface underneath but is severely strained. The final graphene layer is obtained by a 30° rotation of the carbon layer relative to the substrate. (d) The simulated STM image of the $(6\sqrt{3}\times 6\sqrt{3})R30°$ surface.

View Article Online

Published on 03 February 2015. Downloaded by Changchun Institute of Optics, Fine Mechanics and Physics, CAS on 29/05/2016 11:47:40.

Si–C flips. The qualitative agreement between experimental and simulated STM images confirms the random origin of the intermediate surface structures.

When all C atoms in the top Si–C bilayer of SiC(0001) flipped down, the second Si–C bilayer will be replaced by a single carbon layer in which C atoms bond alternatively to the Si atoms below, resulting in a commensurate (1 × 1) reconstruction, as shown in Fig. 3(c). However, in such a configuration, the C–C bond length is about 1.80 Å, much longer than 1.42 Å in graphene and 1.54 Å in diamond. This means that the carbon layer is severely strained, as previously reported.[46] To release the mechanical strain, the carbon layer rotates by 30° to form graphene with a unit cell such that every 13 × 13 units of graphene match the $6\sqrt{3} \times 6\sqrt{3}$ unit of the SiC surface underneath, as illustrated in Fig. 3(c) and the simulated STM image shown in Fig. 3(d). The detailed explanation of this structure can be found in our previous paper,[46] which is also consistent with the "Layer 1" shown in Fig. 3(a) reported by Norimatsu *et al.*[47]

With this flip mechanism, a monolayer graphene can be grown on SiC along a route to unravel the SiC sp^3 lattice through the lowest energy barriers: (1) the creation of surface V_{Si} which requires an energy of 7.46 eV if assisted by the $(\sqrt{3} \times \sqrt{3})R30°$ surface reconstruction or 8.00 eV for the unreconstructed 1 × 1 surface, (2) flipping of the Si–C pair assisted by a Si vacancy which requires an energy of 2.4 eV, (3) sublimation of Si atoms from the Si chain in the top layer, requiring 5.5 eV for the central one and 5.7 eV for the other two and the formation of the C_4 cluster in the second layer, (4) propagation of Si sublimation, at an energy cost of about 5.6 eV and aggregation of C atoms into a graphene flake, (5) delamination of carbon nanoflakes from the SiC layer below and a 30° rotation to release mechanical strain, and formation of the $(6\sqrt{3} \times 6\sqrt{3})R30°$ structure. In this process of dynamic growth of graphene on SiC, Si sublimation requires the most energy to break the Si–C or the Si–Si bonds, which accounts for the high growth temperature of >1000 °C on a global heating substrate. Furthermore, since the final delamination of graphene sheets requires a rotation of 30° relative to the SiC(0001) surface underneath and the graphene domains are free to rotate with respect to one another, the final product would consist of domains with limited sizes and random orientations if the initial sublimation of Si atoms takes place randomly.

3.3. Energetic-beam enhanced growth

Based on the Si–C bond flipping growth mechanism, various critical stages during growth take place at different energy costs. This may lead to strategies based on energy control for more efficient graphene growth on SiC. We propose the following.

(i) The growth temperature can be significantly reduced provided that breaking of Si–C and Si–Si bonds during Si sublimation can be assisted by other mechanisms, such as energetic electron or laser beam irradiation instead of thermal excitation.[21–24] Moreover, other nanofabrication and patterning technologies which can cause the sputtering of substrate atoms with a high spatial resolution, such as a focused ion beam (FIB) and plasma etching, are alternatives. FIB offers both high-resolution imaging and flexible micromachining in a single platform.[48] For example, helium ion microscopy with an ultimate resolution of 0.5 nm or better is a recently developed technology which is useful for carbon nanostructure imaging.[49,50] Plasma etching is another suitable technique with atomic precision for graphene growth. Zhao *et al.* have synthesized few-layered graphene by etching graphite using H_2O_2 plasma with optimum parameters.[51] The key etching parameters can be precisely controlled, making it possible to introduce FIB or plasma etching to the SiC substrate for graphene formation.

(ii) The strategy of using an energetic-beam enhanced method instead of a separate heating process could significantly reduce the growth temperature. However, the key parameters of energetic-beams should be precisely controlled to ensure Si sublimation in hierarchical order rather than at random. Well-organized manipulation of Si sublimation by precisely controlling the energy, duration and space distribution of energetic-beams not only eliminates grain boundaries and the random orientation originating from the 30° rotational movement during graphene delamination, but also allows engineering of graphene patterns for specific electric circuits.

On the $(\sqrt{3} \times \sqrt{3})R30°$ surface, the different energy required for sublimation of the 1/3 salient Si atoms and the 2/3 sunken Si atoms allows a high selectivity of Si sublimation sites and areas by precise control of the energy of energetic-beams, as schematically shown in Fig. 4(a) and (b). In the presence of V_{Si}s, created by the energetic-beam, the flipping of Si–C pairs can progress by thermal excitation at a low temperature, as shown in Fig. 4(c). Immediately after the bond flipping, Fig. 4(d) shows that the swapped atoms Si_i and their

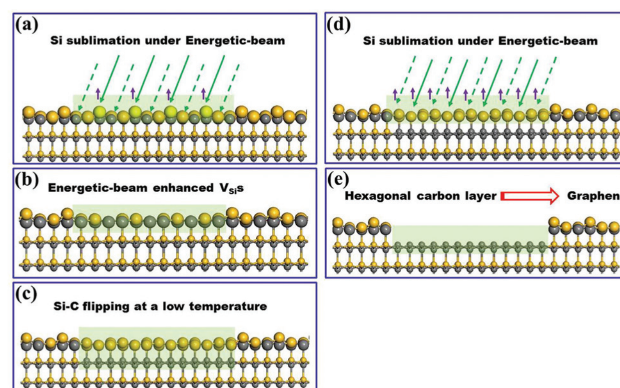

Fig. 4 Proposed energetic-beam controlled growth of high-quality graphene on the SiC (0001) surface. (a) Destabilization of Si_3 type Si atoms in the surface layer with the energetic-beam of right energy. (b) Surface structure with Si vacancies, after sublimation of Si_3 type atoms. (c) Si vacancy induced Si–C bond flipping. (d) Removal of swapped Si atoms and residual Si atoms from the top layer. (e) Formation of a strained layer of carbon. Rotation of the carbon layer relative to the substrate and bond contraction led to the formation of the graphene layer. The yellow and gray balls represent Si and C atoms, respectively.

This journal is © The Royal Society of Chemistry 2015

Published on 03 February 2015. Downloaded by Changchun Institute of Optics, Fine Mechanics and Physics, CAS on 29/05/2016 11:47:40.

neighbors Si_j sublimate under a lower energy energetic-beam with respect to Fig. 4(a), leaving a single layer of carbon atoms which finally delaminates from the substrate with an overall rotation of 30°. Since the C–C bond is much stronger than the C–Si and Si–Si bonds (3.7, 3.21, and 2.34 eV, respectively, in amorphous hydrogenated SiC alloys[52]), the projecting beam with optimized energy will prompt Si sublimation without harming the C–C bonds below. Precisely controlling the energy, duration, and space distribution of energetic-beams in the dynamic process may lead to the desired graphene patterns with tunable width and length at a significantly low temperature.

4. Conclusion

In conclusion, based on our DFT calculations, we described a complete dynamic growth process of graphene on SiC(0001), which starts from a silicon vacancy at the surface, goes through the SiC surface sp^3 lattice be unravelled along the minimum energy path of flipping of Si–C pairs, sublimation of Si atoms, formation of the C clusters, propagating of Si sublimation, aggregating of C atoms into a graphene flake, and eventually delamination and rotation of monolayer graphene forming the $(6\sqrt{3} \times 6\sqrt{3})R30°$ surface. The identified energy intervals at various growth stages of graphene on SiC actually ensure an optimized energetic-beam enhanced growth for fabricating graphene with the desired size and patterns at a much lower temperature.

Acknowledgements

L.L. acknowledges the support from the 100 Talents Program of the Chinese Academy of Sciences and the National Natural Science Foundation of China (no. 11174273). X.C. acknowledges the support from the College of Arts and Sciences, University of Missouri – Kansas City.

References

1 K. S. Novoselov, A. K. Geim, S. Morozov, D. Jiang, Y. Zhang, S. Dubonos, *et al.*, *Science*, 2004, **306**, 666–669.
2 K. S. Novoselov, D. Jiang, F. Schedin, T. J. Booth, V. V. Khotkevich, S. V. Morozov, *et al.*, *Proc. Natl. Acad. Sci. U. S. A.*, 2005, **102**, 10451–10453.
3 K. S. Novoselov, V. Fal, L. Colombo, P. Gellert, M. Schwab, K. Kim, *et al.*, *Nature*, 2012, **490**, 192–200.
4 V. Apalkov and M. I. Stockman, *Light: Sci. Appl.*, 2014, **3**, e191.
5 N. Papasimakis, S. Thongrattanasiri, N. I. Zheludev and F. G. de Abajo, *Light: Sci. Appl.*, 2013, **2**, e78.
6 L. Gao, W. Ren, H. Xu, L. Jin, Z. Wang, T. Ma, *et al.*, *Nat. Commun.*, 2012, **3**, 699.
7 C.-M. Seah, S.-P. Chai and A. R. Mohamed, *Carbon*, 2014, **70**, 1–21.
8 S. Stankovich, D. A. Dikin, R. D. Piner, K. A. Kohlhaas, A. Kleinhammes, Y. Jia, *et al.*, *Carbon*, 2007, **45**, 1558–1565.
9 V. C. Tung, M. J. Allen, Y. Yang and R. B. Kaner, *Nat. Nanotechnol.*, 2008, **4**, 25–29.
10 K. V. Emtsev, A. Bostwick, K. Horn, J. Jobst, G. L. Kellogg, L. Ley, *et al.*, *Nat. Mater.*, 2009, **8**, 203–207.
11 W. A. de Heer, C. Berger, M. Ruan, M. Sprinkle, X. Li, Y. Hu, *et al.*, *Proc. Natl. Acad. Sci. U. S. A.*, 2011, **108**, 16900–16905.
12 A. Ouerghi, M. G. Silly, M. Marangolo, C. Mathieu, M. Eddrief, M. Picher, *et al.*, *ACS Nano*, 2012, **6**, 6075–6082.
13 B. Gupta, M. Notarianni, N. Mishra, M. Shafiei, F. Iacopi and N. Motta, *Carbon*, 2014, **68**, 563–572.
14 J. Chen, Y. Wen, Y. Guo, B. Wu, L. Huang, Y. Xue, *et al.*, *J. Am. Chem. Soc.*, 2011, **133**, 17548–17551.
15 J. Kang, S. Hwang, J. H. Kim, M. H. Kim, J. Ryu, S. J. Seo, *et al.*, *ACS Nano*, 2012, **6**, 5360–5365.
16 A. Van Bommel, J. Crombeen and A. Van Tooren, *Surf. Sci.*, 1975, **48**, 463–472.
17 M. Sprinkle, M. Ruan, Y. Hu, J. Hankinson, M. Rubio-Roy, B. Zhang, *et al.*, *Nat. Nanotechnol.*, 2010, **5**, 727–731.
18 J. Baringhaus, M. Ruan, F. Edler, A. Tejeda, M. Sicot and A. Taleb-Ibrahimi, *et al.*, *Nature*, 2014, **506**, 349–356.
19 M. L. Huggins, *J. Am. Chem. Soc.*, 1953, **75**, 4123–4126.
20 Q. Huang, X. Chen, J. Liu, W. Wang, G. Wang, W. Wang, *et al.*, *Chem. Commun.*, 2010, **46**, 4917–4919.
21 H. Go, J. Kwak, Y. Jeon, S.-D. Kim, B. C. Lee, H. S. Kang, *et al.*, *Appl. Phys. Lett.*, 2012, **101**, 092105.
22 P. Dharmaraj, K. Jeganathan, V. Gokulakrishnan, P. Sundara Venkatesh, R. Parameshwari, V. Ramakrishnan, *et al.*, *J. Phys. Chem. C*, 2013, **117**, 19195–19202.
23 S. Lee, M. F. Toney, W. Ko, J. C. Randel, H. J. Jung, K. Munakata, *et al.*, *ACS Nano*, 2010, **4**, 7524–7530.
24 S. N. Yannopoulos, A. Siokou, N. K. Nasikas, V. Dracopoulos, F. Ravani and G. N. Papatheodorou, *Adv. Funct. Mater.*, 2012, **22**, 113–120.
25 W. Chen, H. Xu, L. Liu, X. Gao, D. Qi, G. Peng, *et al.*, *Surf. Sci.*, 2005, **596**, 176–186.
26 K. Emtsev, F. Speck, T. Seyller, L. Ley and J. Riley, *Phys. Rev. B: Condens. Matter*, 2008, **77**, 155303.
27 H. Huang, W. Chen, S. Chen and A. T. S. Wee, *ACS Nano*, 2008, **2**, 2513–2518.
28 J. Hannon, M. Copel and R. Tromp, *Phys. Rev. Lett.*, 2011, **107**, 166101.
29 H. Kageshima, H. Hibino, M. Nagase and H. Yamaguchi, *Appl. Phys. Express*, 2009, **2**, 065502.
30 S. Kim, J. Ihm, H. J. Choi and Y.-W. Son, *Phys. Rev. Lett.*, 2008, **100**, 176802.
31 M. Inoue, H. Kageshima, Y. Kangawa and K. Kakimoto, *Phys. Rev. B: Condens. Matter*, 2012, **86**, 085417.
32 H. Kageshima, H. Hibino, H. Yamaguchi and M. Nagase, *Phys. Rev. B: Condens. Matter*, 2013, **88**, 235405.
33 M. Morita, W. Norimatsu, H.-J. Qian, S. Irle and M. Kusunoki, *Appl. Phys. Lett.*, 2013, **103**, 141602.
34 H. J. Hwang, C. Cho, S. K. Lim, S. Y. Lee, C. G. Kang, H. Hwang, *et al.*, *Appl. Phys. Lett.*, 2011, **99**, 082111.
35 J. P. Perdew, K. Burke and M. Ernzerhof, *Phys. Rev. Lett.*, 1996, **77**, 3865.

Published on 03 February 2015. Downloaded by Changchun Institute of Optics, Fine Mechanics and Physics, CAS on 29/05/2016 11:47:40.

36 G. Kresse and J. Hafner, *Phys. Rev. B: Condens. Matter*, 1993, **47**, 558.
37 G. Kresse and D. Joubert, *Phys. Rev. B: Condens. Matter*, 1999, **59**, 1758.
38 R. Munro, *J. Phys. Chem. Ref. Data*, 1997, **26**, 1195–1203.
39 M. Sabisch, P. Krüger and J. Pollmann, *Phys. Rev. B: Condens. Matter*, 1997, **55**, 10561.
40 V. Bermudez, *Appl. Surf. Sci.*, 1995, **84**, 45–63.
41 F. Owman and P. Mårtensson, *Surf. Sci.*, 1995, **330**, L639–L645.
42 D. Haneman, *Phys. Rev.*, 1961, **121**, 1093.
43 J. Tersoff and D. Hamann, *Scanning Tunneling Microscopy*, Springer, 1993, pp. 59–67.
44 S. W. Poon, W. Chen, E. S. Tok and A. T. Wee, *Appl. Phys. Lett.*, 2008, **92**, 104102.
45 S. W. Poon, W. Chen, A. T. Wee and E. S. Tok, *Phys. Chem. Chem. Phys.*, 2010, **12**, 13522–13533.
46 Z. Ni, W. Chen, X. Fan, J. Kuo, T. Yu and A. Wee, et al., *Phys. Rev. B: Condens. Matter*, 2008, **77**, 115416.
47 W. Norimatsu and M. Kusunoki, *Chem. Phys. Lett.*, 2009, **468**, 52–56.
48 C. Volkert and A. Minor, *MRS Bull.*, 2007, **32**, 389–399.
49 D. C. Bell, M. C. Lemme, L. A. Stern, J. R. Williams and C. M. Marcus, *Nanotechnology*, 2009, **20**, 455301.
50 A. N. Abbas, G. Liu, B. Liu, L. Zhang, H. Liu, D. Ohlberg, *et al.*, *ACS Nano*, 2014, **8**, 1538–1546.
51 G. Zhao, D. Shao, C. Chen and X. Wang, *Appl. Phys. Lett.*, 2011, **98**, 183114–183114.
52 H. Efstathiadis, Z. Yin and F. Smith, *Phys. Rev. B: Condens. Matter*, 1992, **46**, 13119.

This journal is © The Royal Society of Chemistry 2015